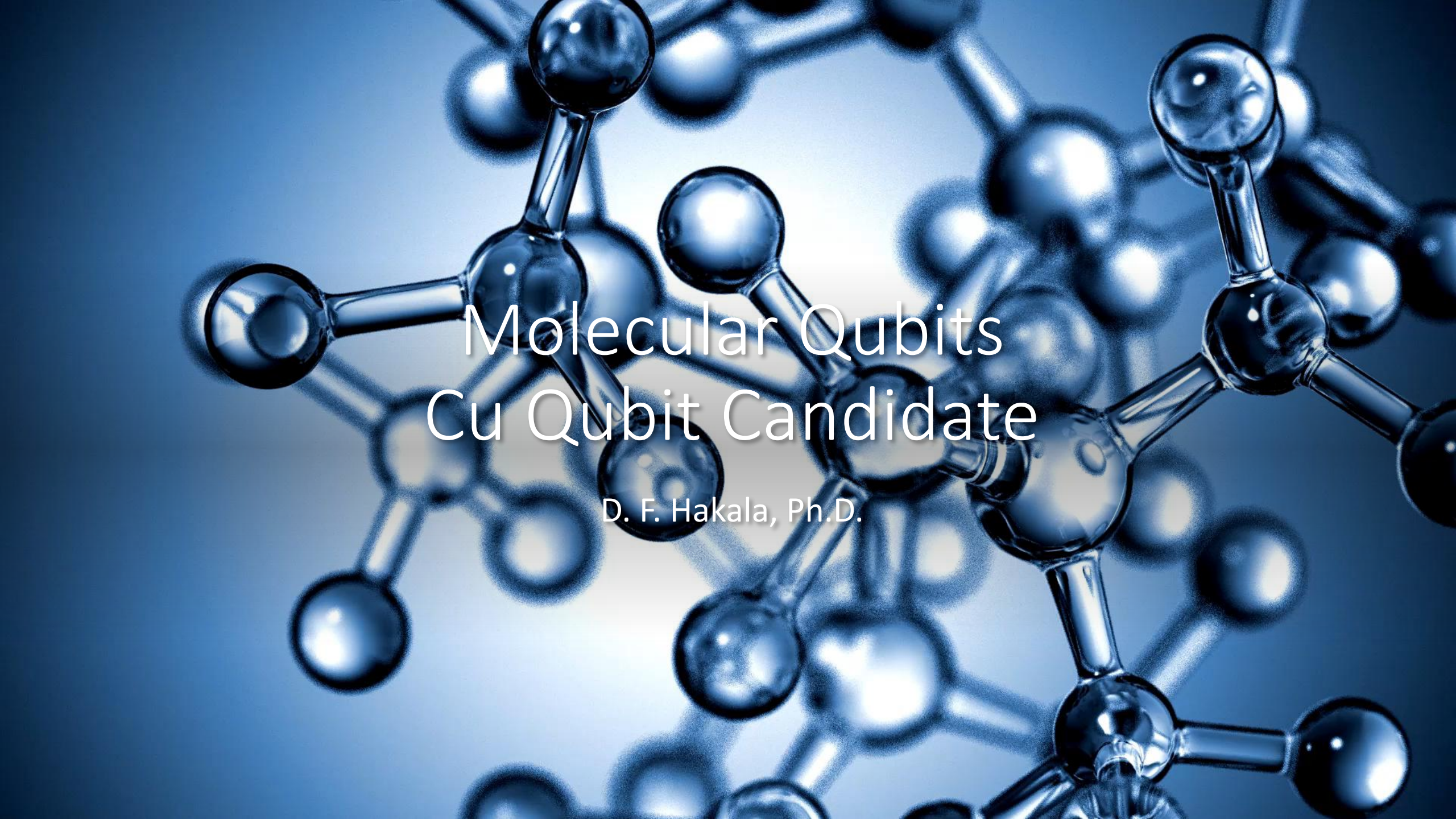

Molecular Qubits
Cu Qubit Candidate

D. F. Hakala, Ph.D.

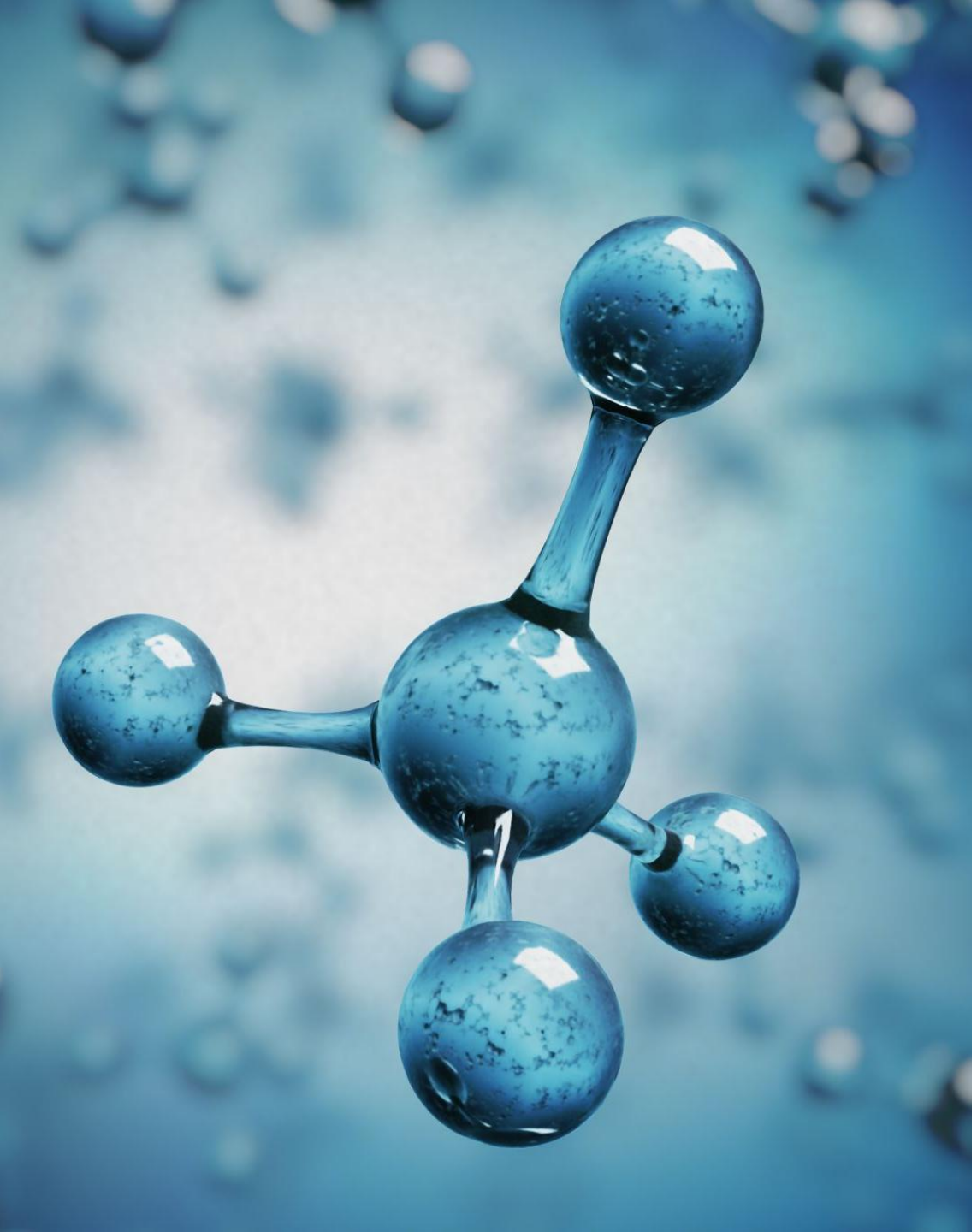

Introduction-Molecular Qubits

- A good relatively recent review related to molecular qubits is
- **Recent Innovations in Solid-State and Molecular Qubits for Quantum Information Applications**

  J. Phys. Chem. Lett. 2021, 12, 10742-10745
- There are over 40 references in this article, many of them with respect to molecular qubits.
- This is an overview for a Virtual Issue of J. Phys .Chem.Lett. on this subject.

Bloch Sphere Representation of the Qubit

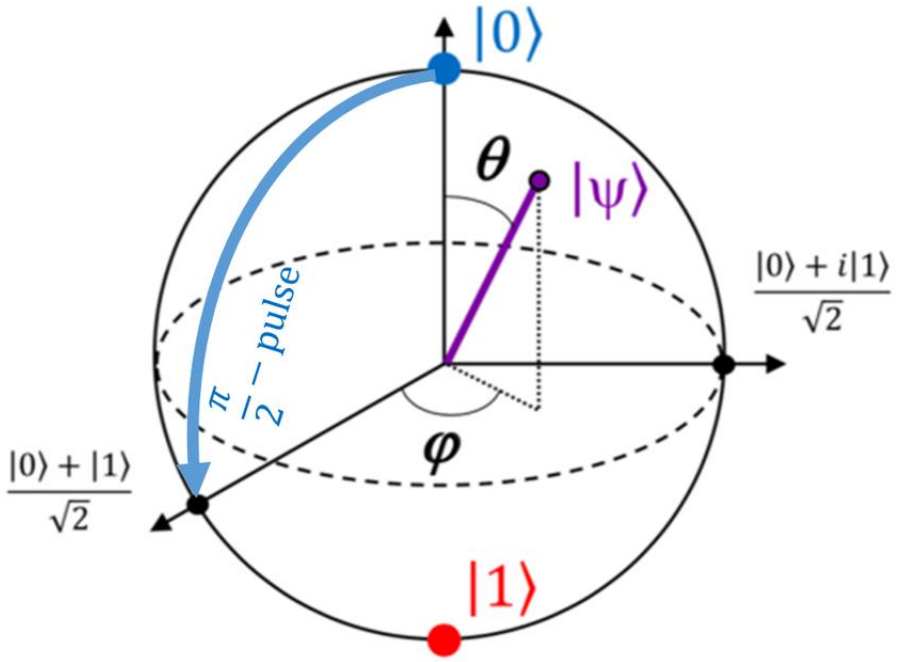

$$|\psi\rangle = cos\frac{\theta}{2}|0\rangle + e^{i\varphi}sin\frac{\theta}{2}|1\rangle$$

Applying (typically) microwave pulses of the correct time and frequency(it will need to be at the resonance of the energy difference between the |0> and |1> states at the applied magnetic field strength) will rotate the qubit from its initial orientation to a final one.

Assume the qubit is initially in the |0> state (theta =0). A resonant frequency pulse of theta=Pi/2 will rotate the qubit 90 degrees on the block sphere and result in a superposition (equal weights) of the |0> and |1> states or a normalized state of $(|0\rangle+|1\rangle)/2^{1/2}$. A pulse of length theta=Pi would change the qubit from the |0> state to the |1> state, effectively a NOT gate.

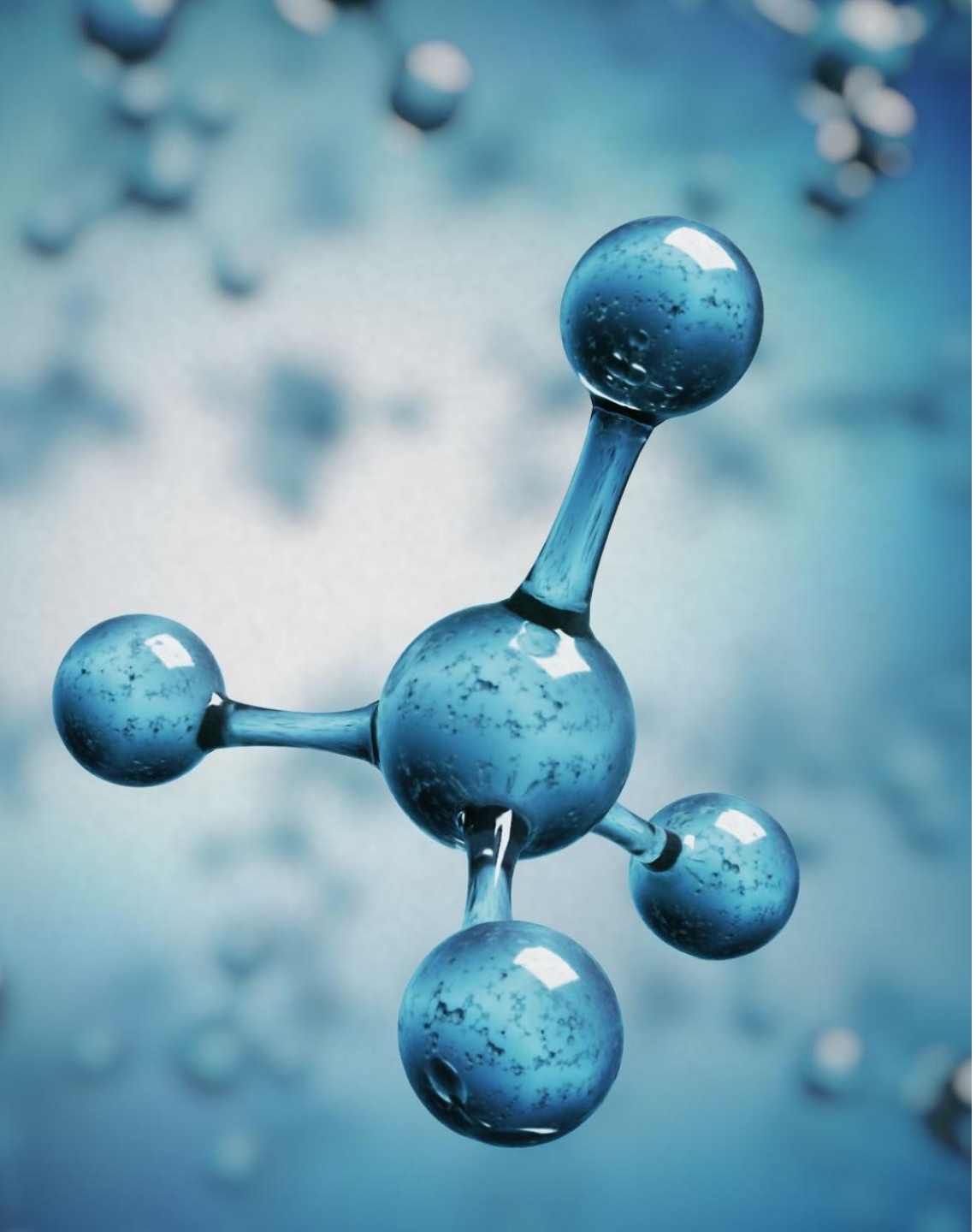

Molecular Qubits

- A qubit is an object that has two states (generally referred to as |0> and |1>) and all their superpositions. There are many possible physical implementations of the qubit. One of these that is attractive is the molecular qubit.
- The attractiveness is for several reasons.
  - They are small which will help in scaling up to higher device densities
  - They can be engineered or designed with respect to a number of different properties.
  - They are capable of being encoded, addressed, manipulated, and read by means such as optical or microwave radiation.
- A typical molecular qubit is one that is spin based using the spin of unpaired electron(s). This energy of the molecule will both change and split in response to an applied magnetic field.

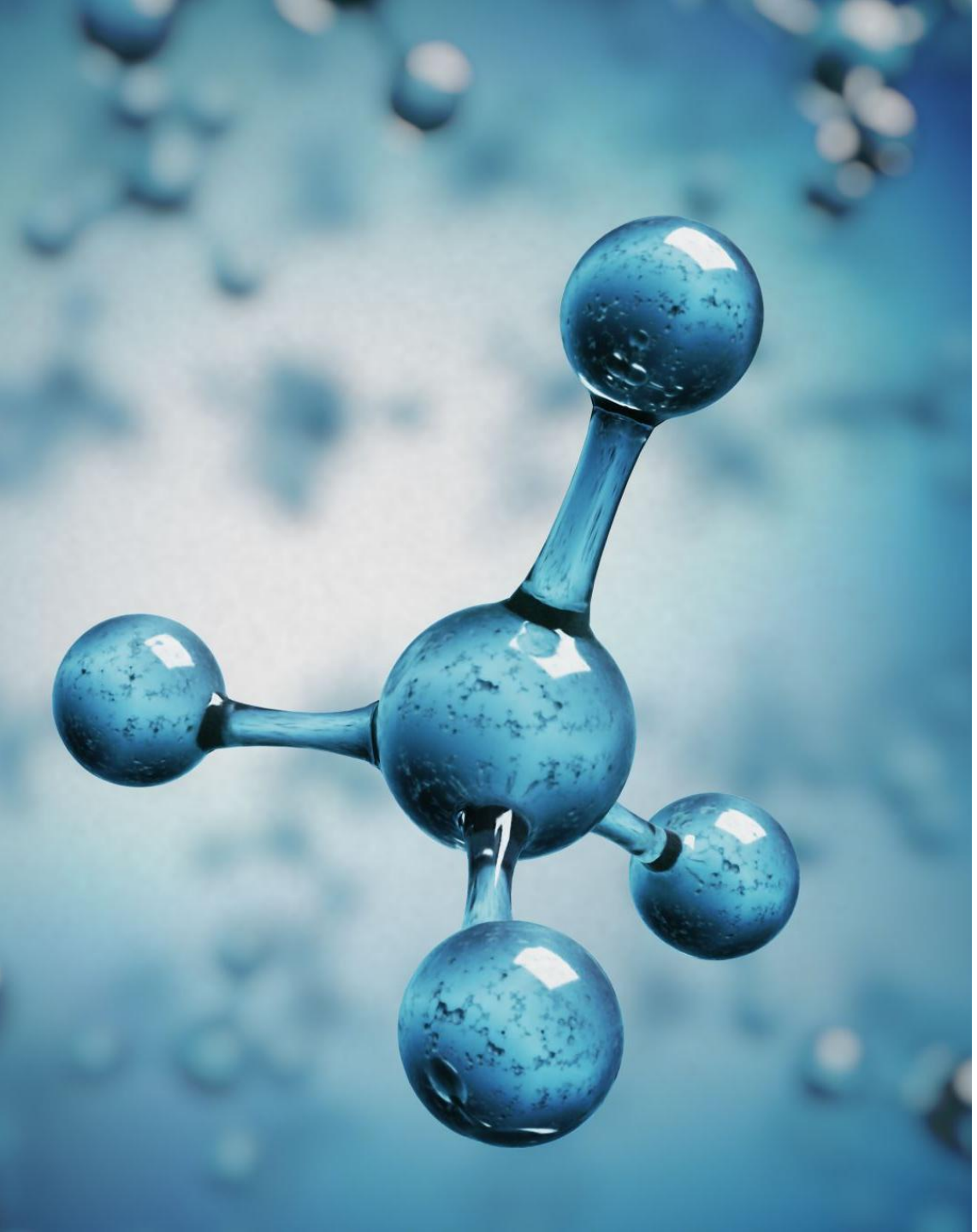

Molecular Qubits

- So, one of the characteristics we want in a molecular spin qubit is that it is easy to achieve a spin state. Coordination compounds of transition metals such as Cr, Cu, Ni, V etc. can be selected to have unpaired spins.
- Another characteristic is that we want to maximize the time it can spend in the targeted coherent superpositions of qubits. Since there can be an I* S interaction between nuclear spins (I) and the electron spin (S) of the transition metal , this interaction can result in a decoherence of the qubit state. By designing molecular qubits such that atoms with net or strong nuclear spins are further from the transition metal atom we should improve the coherence time of the qubit.
- The stiffness of the lattice can also be a factor. A stiffer lattice generally means higher phonon energies. The higher energies are less likely to interact and cause decoherence of the qubit.
- Qubits that have better coherence times at high temperatures are of interest because this could result in a less costly quantum computer. So good room temperature coherence is a desired objective. However, even good coherence at liquid N2 temperature (77K) would be huge improvement over liquid helium temperatures.

Molecular Qubits

- One type of molecule proposed as a qubit with better room temperature coherence are copper(II) complexes.
    - Room Temperature Quantum Coherence in a Potential Molecular Qubit.

      NATURE COMMUNICATIONS , 5:5304 , DOI: 10.1038/ncomms6304 , www.nature.com/naturecommunications
- An analog for one of these molecules has been studied to better understand the electronic states of the molecule, focusing on the lower lying states which are of most interest in the dynamics of the qubit behavior .
    - Characterizing Excited States of a Copper Based Molecular Qubit Candidate with Correlated Electronic Structure Methods.

      J. Phys. Chem. A 2023, 127, 6764-6770
- The following does initial calculations on the copper qubit analog studied in the last paper.

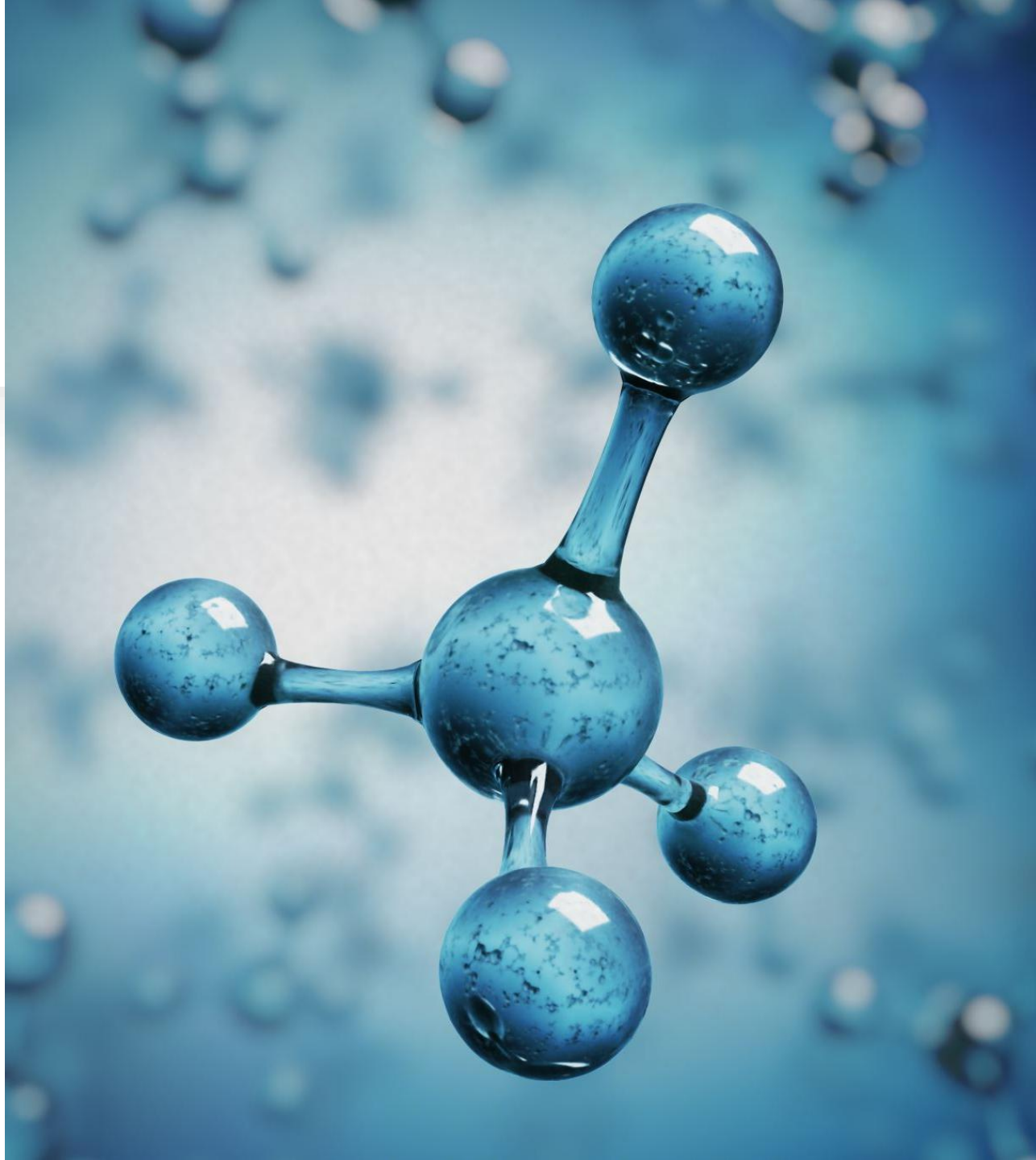

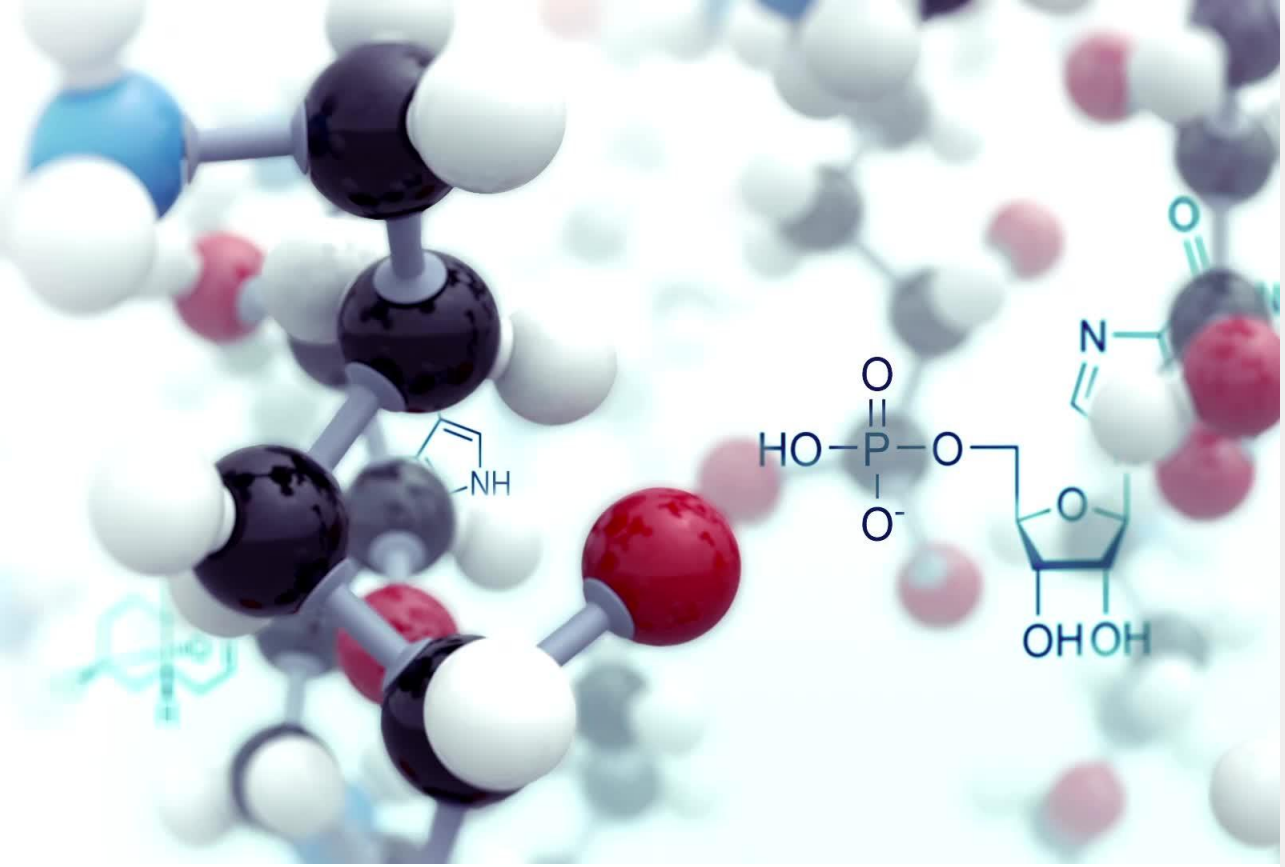

Calculations

- The molecule examined is an analog for a proposed room temperature molecular qubit. $[Cu(II)S_4C_4H_4]^{-2}$, or $[Cu(II)(edt)_2]^{-2}$ where edt is short for ethylene dithiolate a doubly negatively charged ligand.
- The Cu qubit analog molecule was geometry optimized using a DFT method with the PBEO functional, a basis set of def2/TZVPPD and the auxillary basis set def2/J.
- The molecule was drawn and initially optimized using Spartan 20.
- The resulting data was used to generate an XYZ file that was edited to be suitable for ORCA.
- The DFT calculation was done using ORCA 5.04.

Cu Qubit Analog

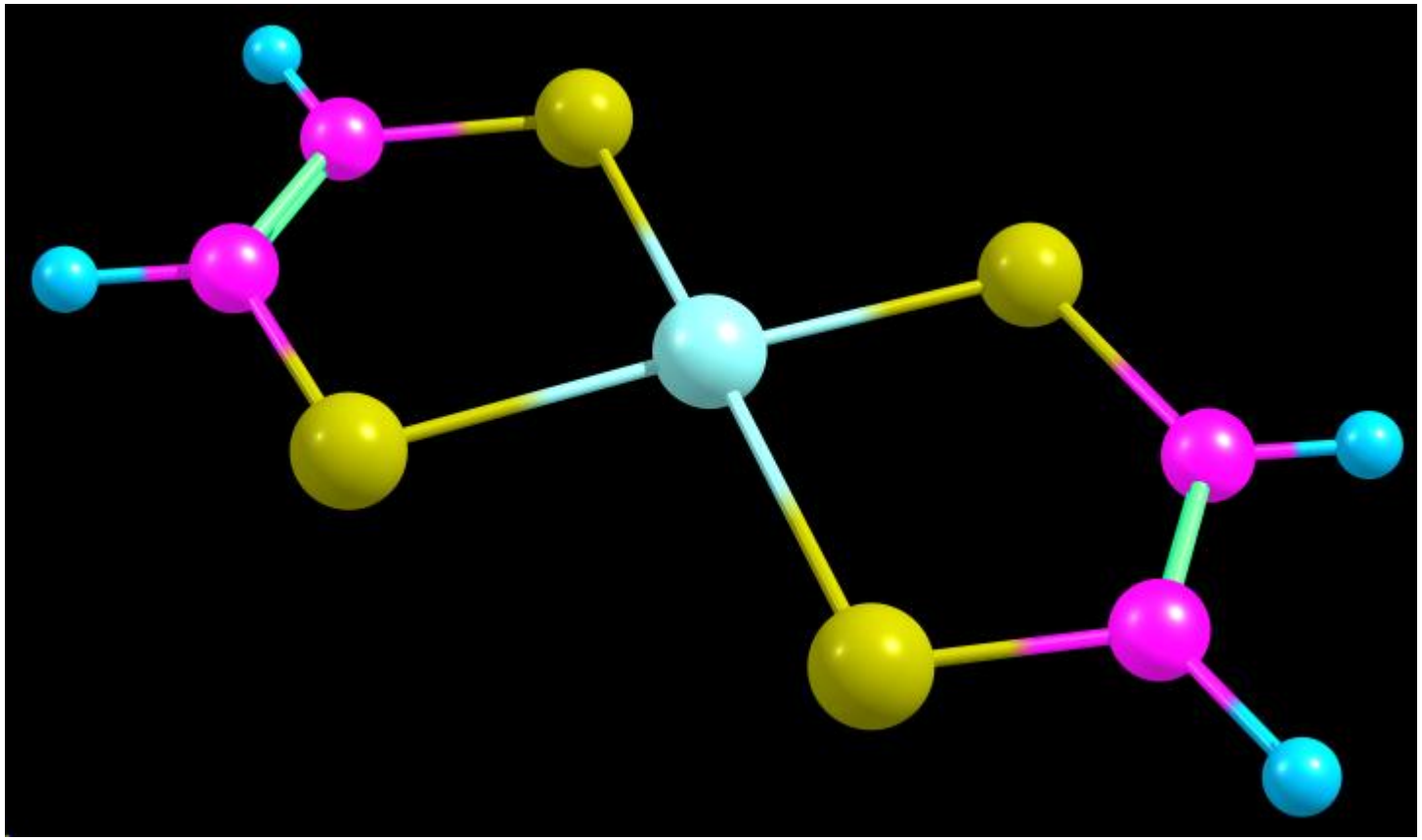

This molecule is an analog for a proposed room temperature molecular qubit. $[Cu(II)S_4C_4H_4]^{-2}$

A proposed molecule to which this is an analog has four cyano groups instead of the four hydrogens. The carbon 12 atoms have no net nuclear spin (as opposed to the hydrogens). The nitrogen has a very weak spin interaction. They therefore will have less interaction with the Cu(II) spin, reducing environmental interaction of the qubit.

However, the addition of additional electrons from the four cyano groups significantly adds computational complexity to quantum calculations, So this molecule is easier to study.

ORCA Input File

```
! PBE0  def2-TZVPPD  def2/J OPT
! PAL8 Printbasis PrintMOs


* xyz -2 2
 Cu      0.79423      0.71870      0.00000
  S     -1.02180      2.16851     -0.00000
  S      2.14846      2.60707     -0.00000
  S      2.61024     -0.73113     -0.00000
  S     -0.55997     -1.16969     -0.00000
  C     -2.35657      0.98041     -0.00000
  C     -2.16717     -0.38861     -0.00000
  C      3.75565      1.82598     -0.00000
  C      3.94504      0.45693     -0.00000
  H      4.95690      0.07356      0.00000
  H      4.62545      2.46965      0.00000
  H     -3.36845      1.36378      0.00000
  H     -3.03696     -1.03230      0.00000
```

This file shows that the ORCA computational chemistry calculation was done using

- A Density Functional Theory (DFT) functional of PBE0
- A basis set of def2-TZVPPD (triple zeta level)
- An auxillary basis set of def2/J

The calculation itself was a geometry optimization (keyword = OPT)

The calculation was done using 8 threads of parallel processing (keyword = PAL8)

The other comments refer to the data printed in the output file to be consistent with what ChemCraft software requires for input to that program for visualization of the Molecular Orbitals.

The atomic position are given by the XYZ file in angstroms

The net charge on the molecule is -2
The multiplicity of 2S+1 is 2, since the spin S is ½.

MO Energy Diagrams from ORCA Output

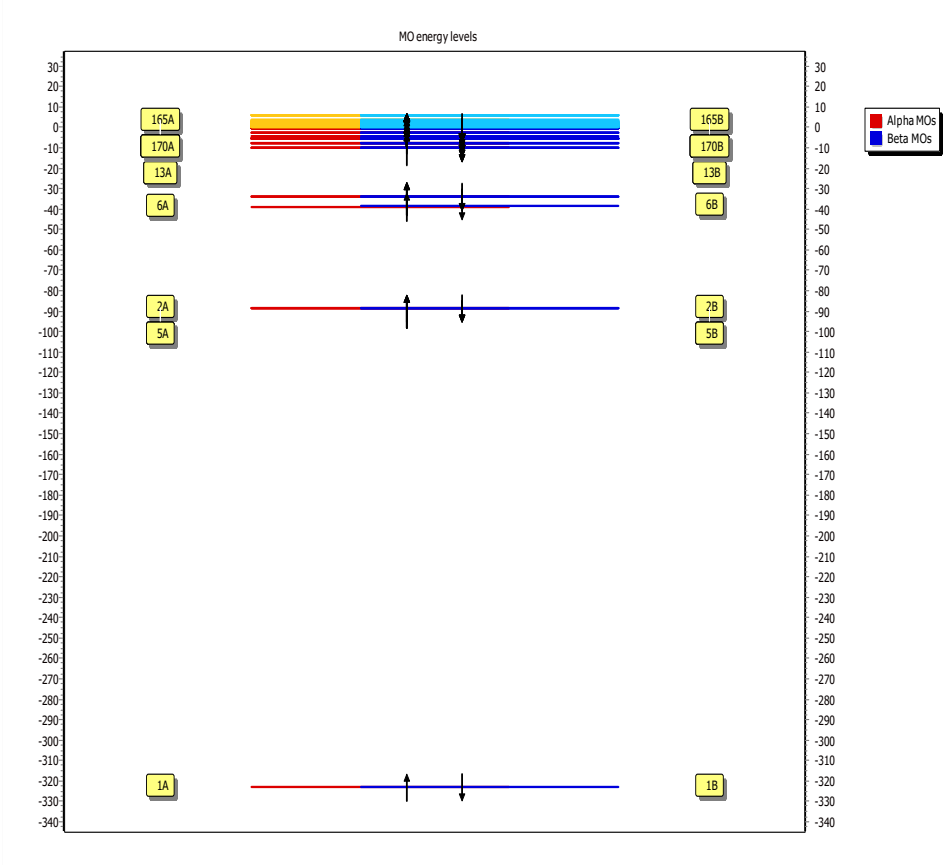

Overall View

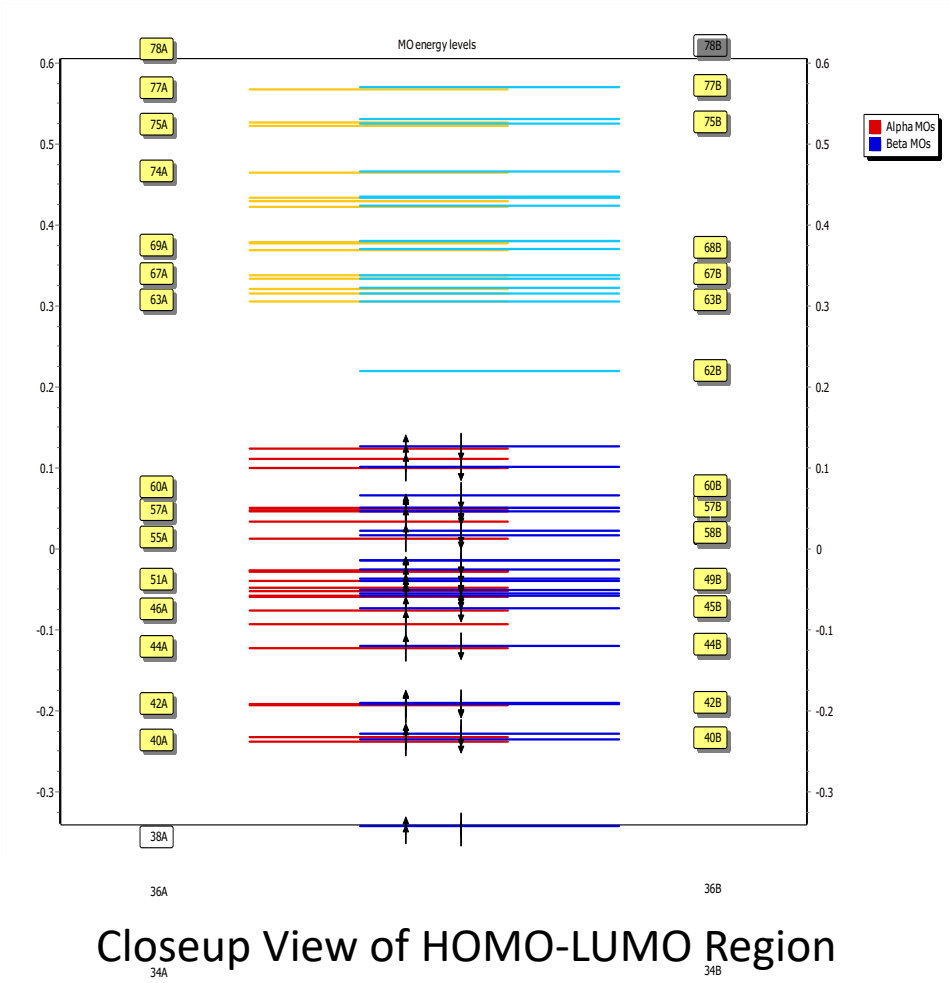

Closeup View of HOMO-LUMO Region

Rendered with ChemCraft

Graphical Representations of Molecular Orbitals

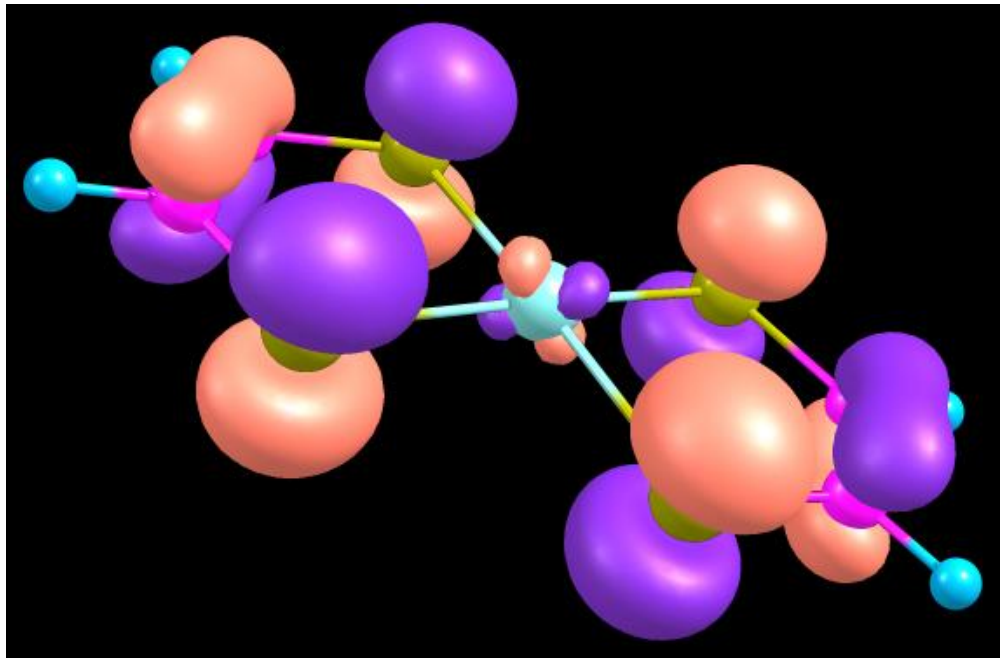

This is the Highest Occupied Molecular Orbital (HOMO) for the Cu(II) molecule as calculated.

Note the d_{xz} character around the Cu atom

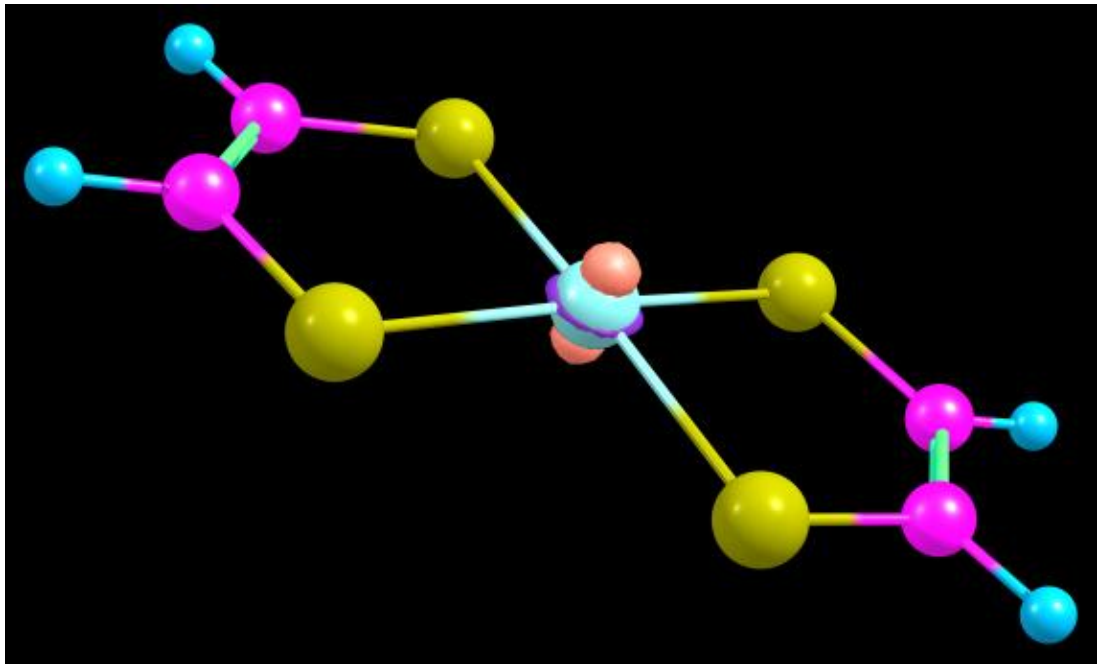

This is the Lowest Unoccupied Molecular Orbital (LUMO) for the Cu(II) molecule as calculated.

Note the d_{z2} character around the Cu atom

Spin Density 3D Isosurface

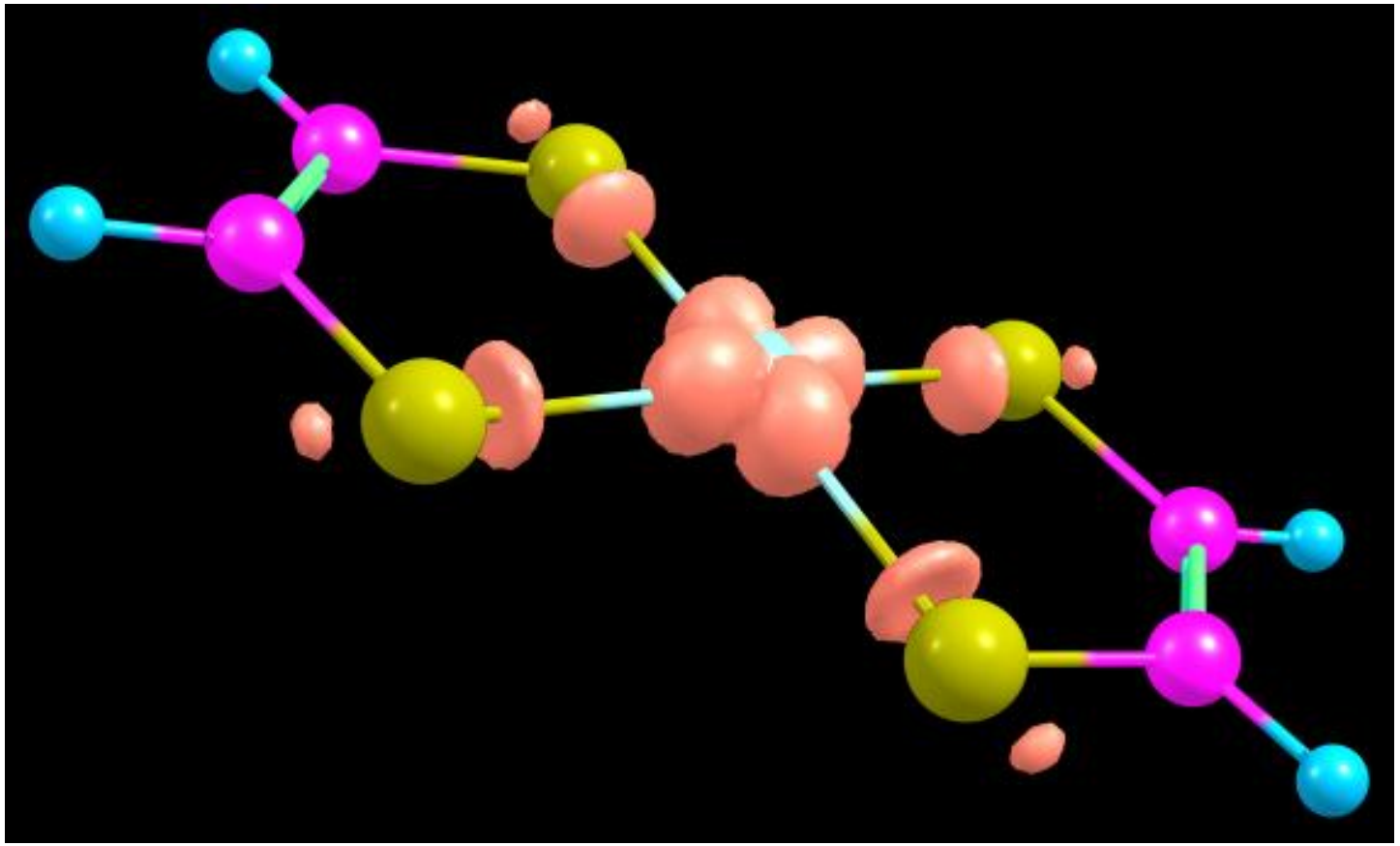

This is the Chemcraft rendering of the spin density of the Cu qubit candidate with hydrogen substitutions.

ABSORPTION SPECTRUM
Cu Qubit Candidate (H Version)
VIA TRANSITION ELECTRIC DIPOLE MOMENTS*

State	Energy (cm-1)	Wavelength (nm)	fosc	T2 (au**2)	TX (au)	TY (au)	TZ (au)
1	8143.4	1228.0	0.000007381	0.00030	0.00193	-0.01717	-0.00000
2	14961.1	668.4	0.000000041	0.00000	-0.00000	-0.00000	0.00096
3	17862.9	559.8	0.000608257	0.01121	-0.10487	-0.01458	0.00000
4	18711.4	534.4	0.000000007	0.00000	0.00001	0.00000	0.00035
5	21058.8	474.9	0.000000000	0.00000	0.00004	0.00002	0.00004
6	22698.8	440.6	0.000333950	0.00484	-0.01340	0.06829	-0.00000
7	25371.2	394.1	0.000000000	0.00000	-0.00000	-0.00002	0.00001
8	25810.8	387.4	0.000279522	0.00357	-0.00808	-0.05916	0.00000
9	26013.1	384.4	0.256247058	3.24297	1.78145	0.26348	-0.00002
10	26124.3	382.8	0.000003534	0.00004	0.00271	0.00040	0.00608

Strongest transition is highlighted

* From ORCA 6.0 TDDFT/TDA Calculation

UV-VIS Calculated Absorption Spectrum Cu Qubit Candidate (H Version)

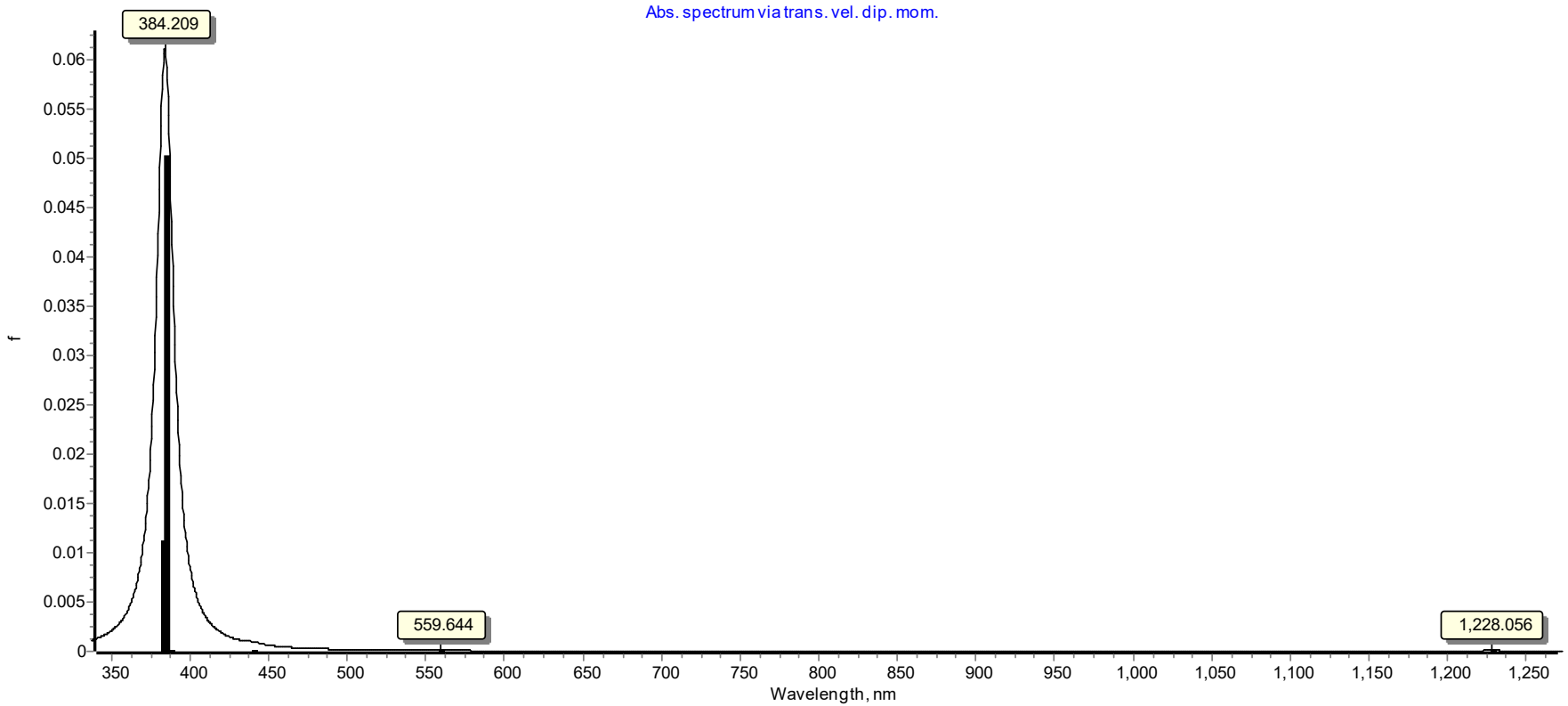

ABSORPTION SPECTRUM
Cu Qubit-Cyano Version
VIA
TRANSITION ELECTRIC DIPOLE MOMENTS*

State	Energy (cm-1)	Wavelength (nm)	fosc	T2 (au^2)	TX (au)	TY (au)	TZ (au)
1	9449.1	1058.3	0.000000001	0.00000	0.00013	-0.00000	0.00000
2	15786.0	633.5	0.000000000	0.00000	-0.00000	-0.00000	0.00000
3	16599.1	602.4	0.000064184	0.00127	0.03568	-0.00000	0.00000
4	17367.2	575.8	0.000000000	0.00000	-0.00000	-0.00000	-0.00000
5	18926.6	528.4	0.000000000	0.00000	-0.00000	0.00000	-0.00000
6	19776.9	505.6	0.000000000	0.00000	0.00000	0.00000	-0.00001
7	20551.2	486.6	0.000000028	0.00000	0.00000	-0.00068	-0.00000
8	22107.1	452.3	0.000000575	0.00001	0.00000	0.00000	-0.00293
9	22860.5	437.4	0.000000005	0.00000	-0.00014	-0.00010	0.00022
10	23715.9	421.7	0.000000000	0.00000	-0.00001	-0.00000	0.00001

Strongest transition highlighted (i.e. largest fosc) *Transition moments calculated using ORCA software

UV-VIS Calculated Absorption Spectrum Cu Qubit Candidate (Cyano Version)

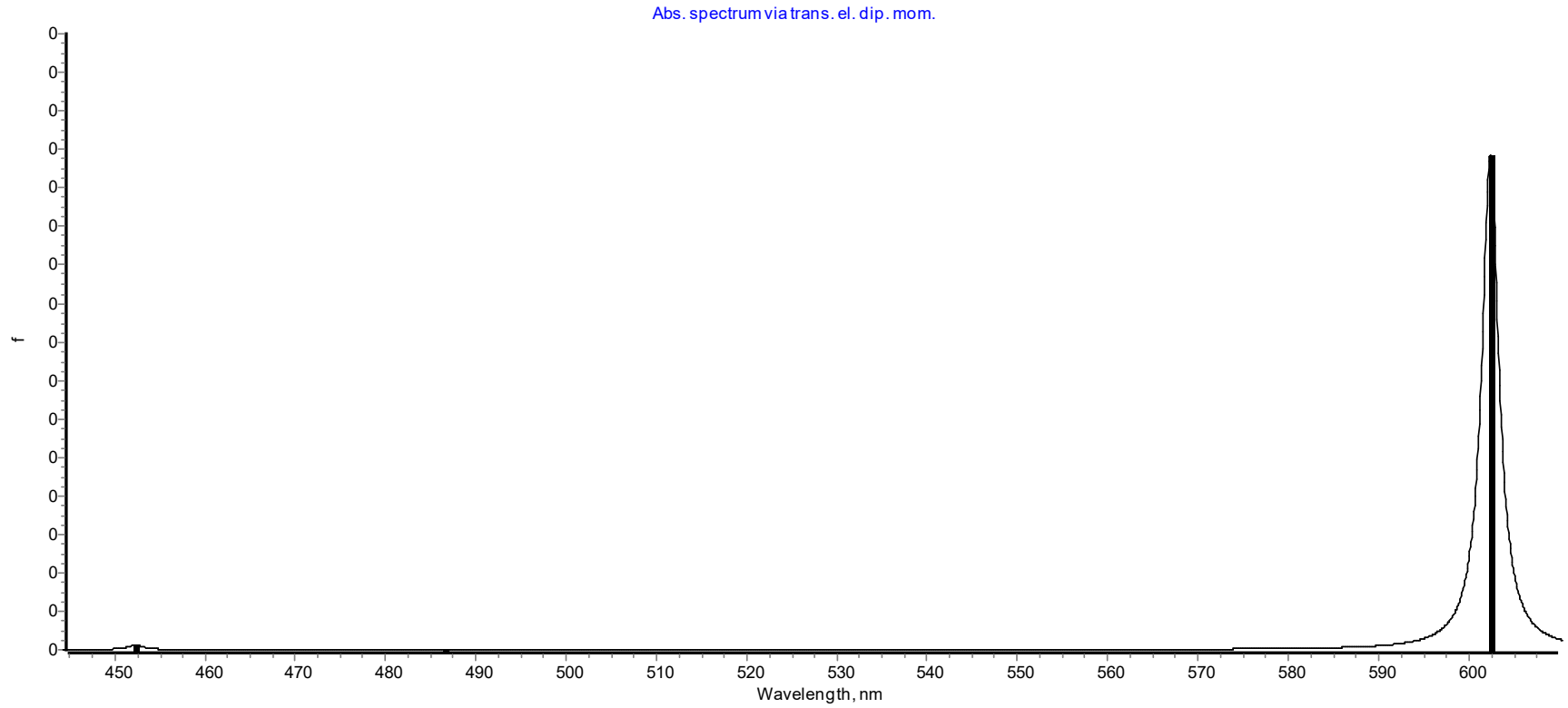

MO’s involved in GS -> State 13 Transition

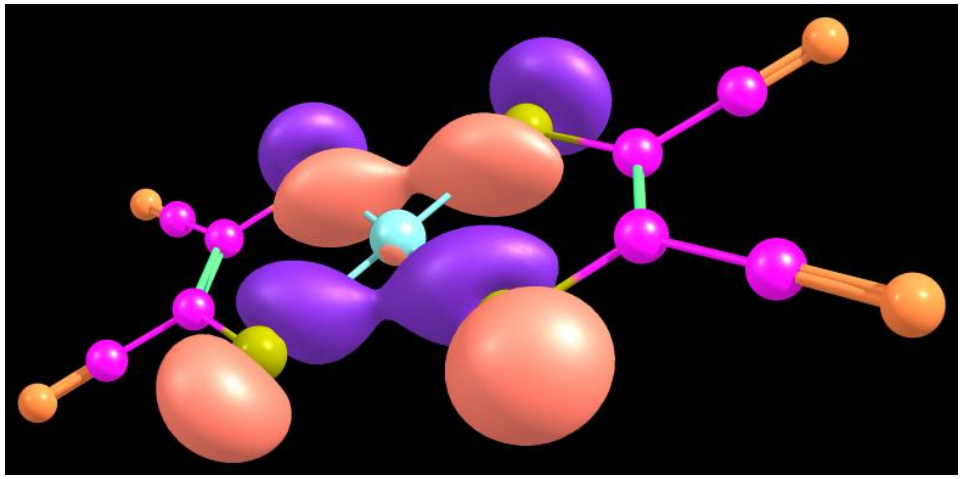

Ground State Molecular Orbitals

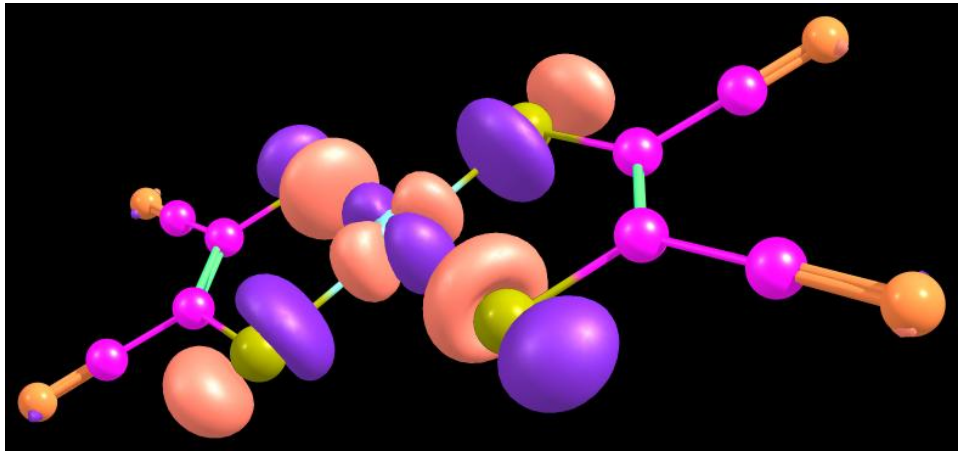

Excited State(State 13) Molecular Orbitals

Spin Density

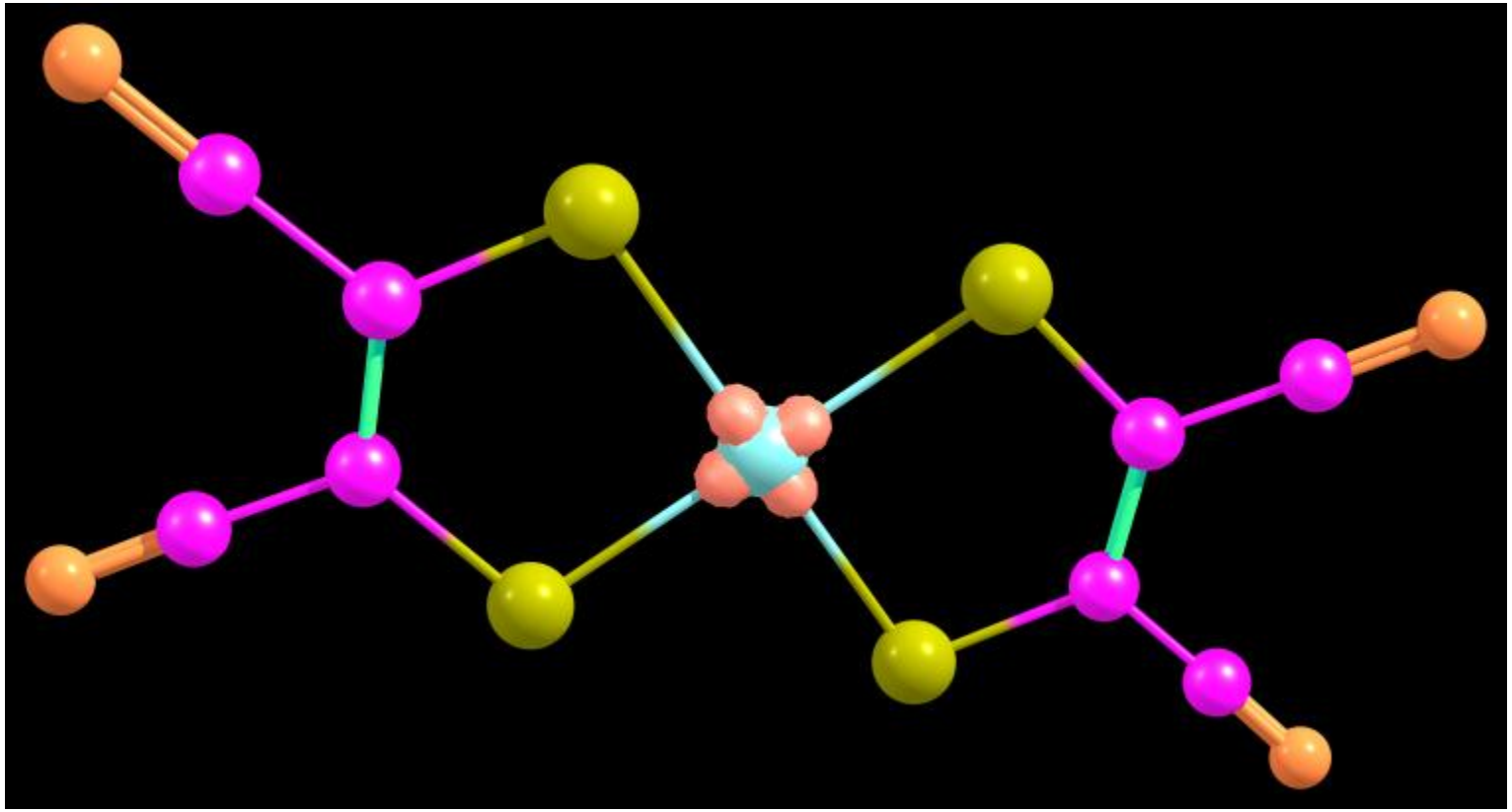

Spin Density Plot of the Cyano Version of the Cu Qubit in the Ground State

(Note: character indicates a dxy configuration around the Cu with the lobes oriented towards the negatively charged Sulfur ligand)

Cu(II) cyano qubit candidate-EPR Spectrum*

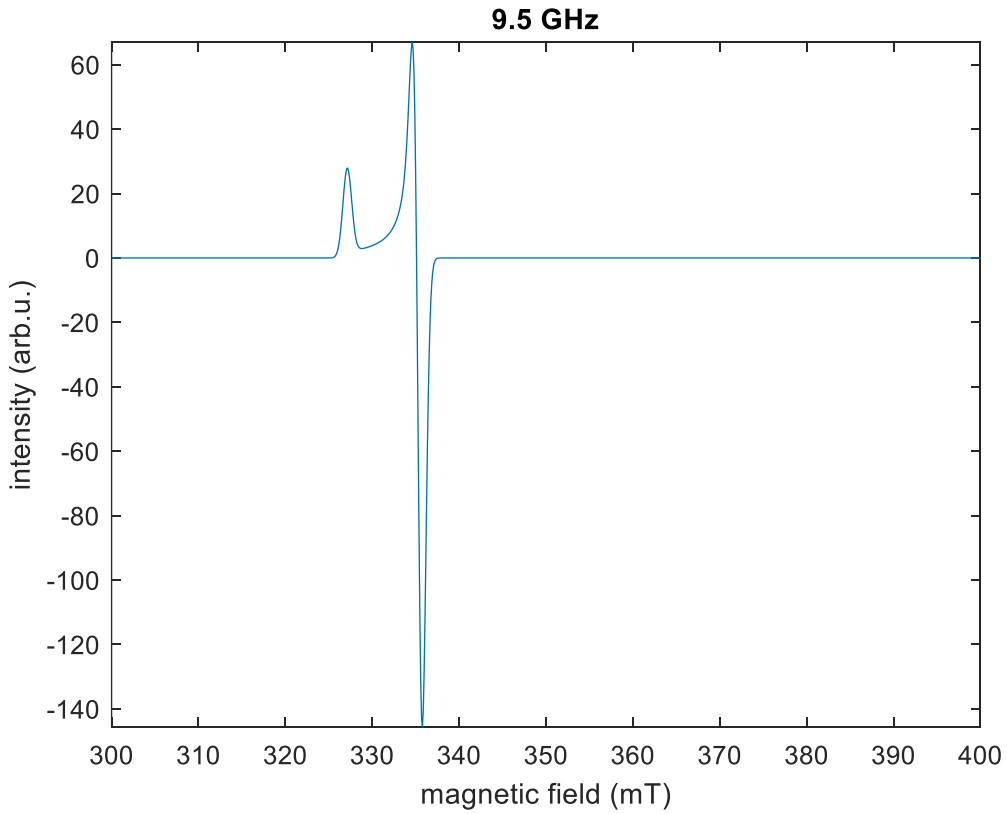

“Pepper”-rigid limit

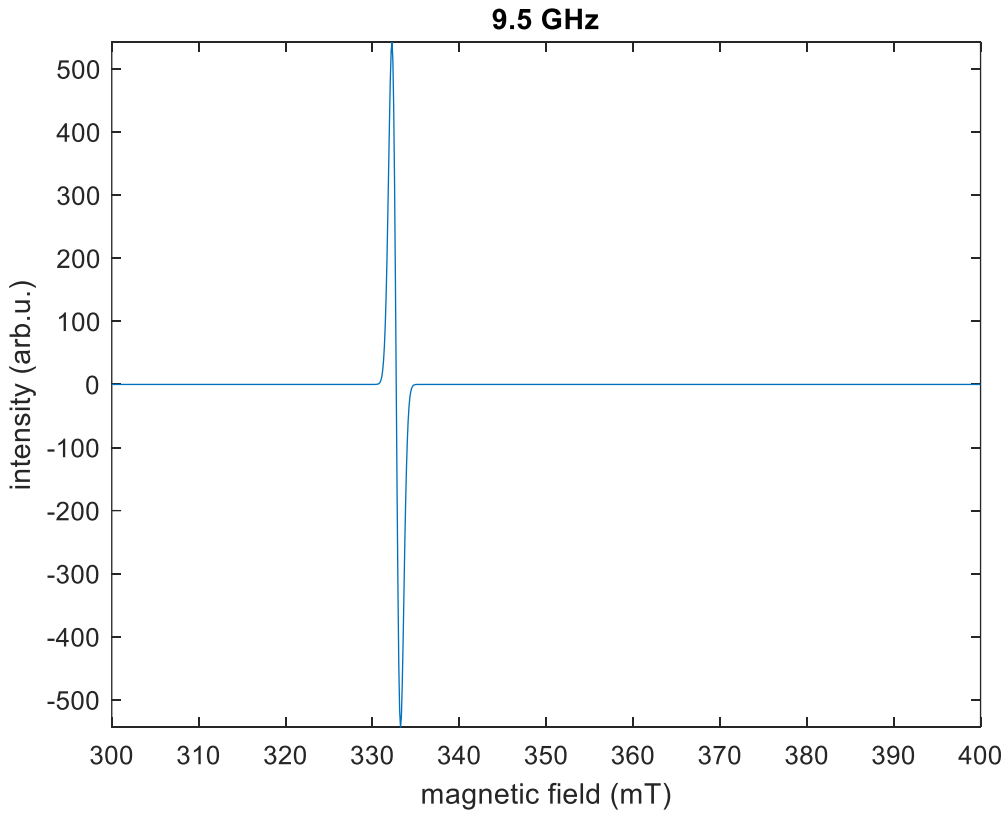

“Garlic”-isotropic limit

* Simulated using Easy Spin on an ORCA 6.0 output file

Cu(II) H qubit candidate-EPR Spectrum*

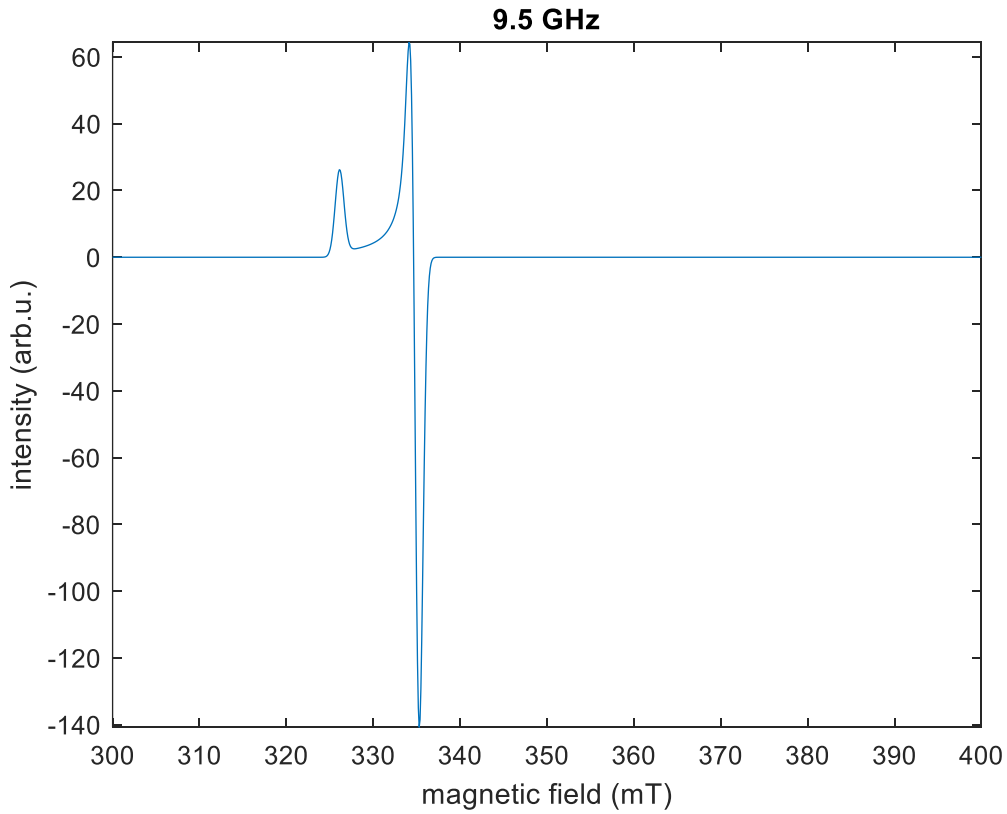

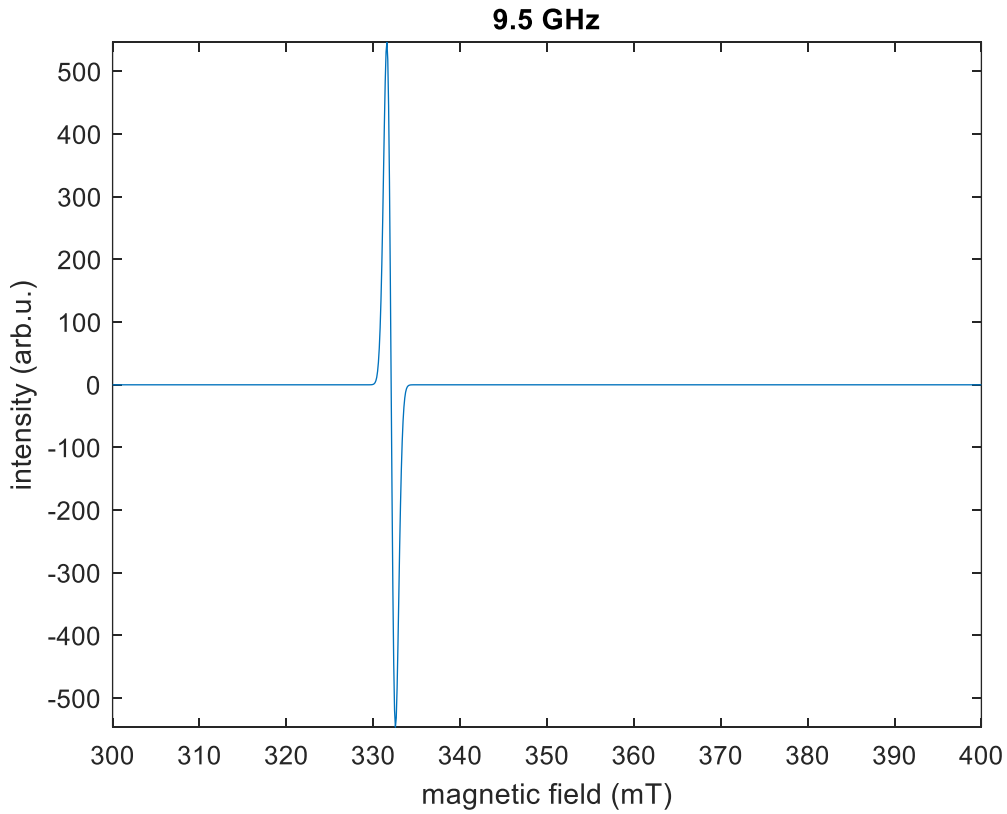

* Simulated using Easy Spin on an ORCA 6.0 output file

Addenda
Room Temperature Copper Qubit Article Extracts

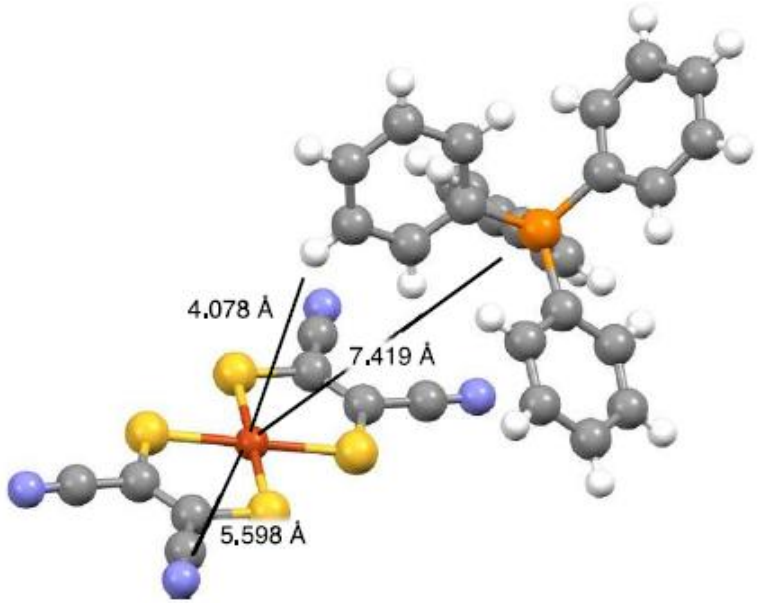

Figure 1 | Structure of 1Cu. Distances between the metal ion and the nearest nuclei with nonzero spins are indicated in Å. Colours: copper-brown, sulfur-yellow, carbon-grey, nitrogen-blue, phosphorus-orange and hydrogen-white.

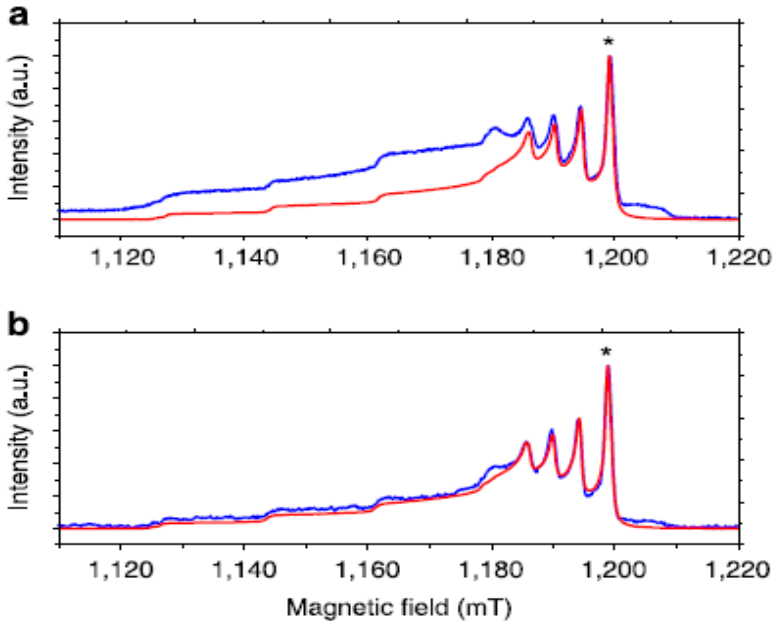

Figure 2 | ESE-detected Q-band EPR spectra of compound $1Cu_{0.001\%}$. Experimental results for EPR spectra (blue) recorded at $T = 7$ K (**a**) and $T = 120$ K (**b**), and simulation (red) using parameters given in the text.

These pictures show extracts from the article about a Room Temperature Cu qubit referred to earlier . Fig.1 shows the structure of the molecule studied and some interatomic distances. The copper is in an essentially square planar geometric configuration. Fig. 2 shows the Electron Paramagnetic Resonance (EPR) spectrum and simulation fits to the spectrum at two different temperatures. The spectrum is shown as a function of the applied magnetic field. Typically, a fixed RF/Microwave frequency is used and as the magnetic field is varied the energy differences go in and out of resonance with the electromagnetic radiation. Spectral finer details are related to the Cu atom spin and its couplings to nuclear spins.

Room Temperature Copper Qubit Article Extracts

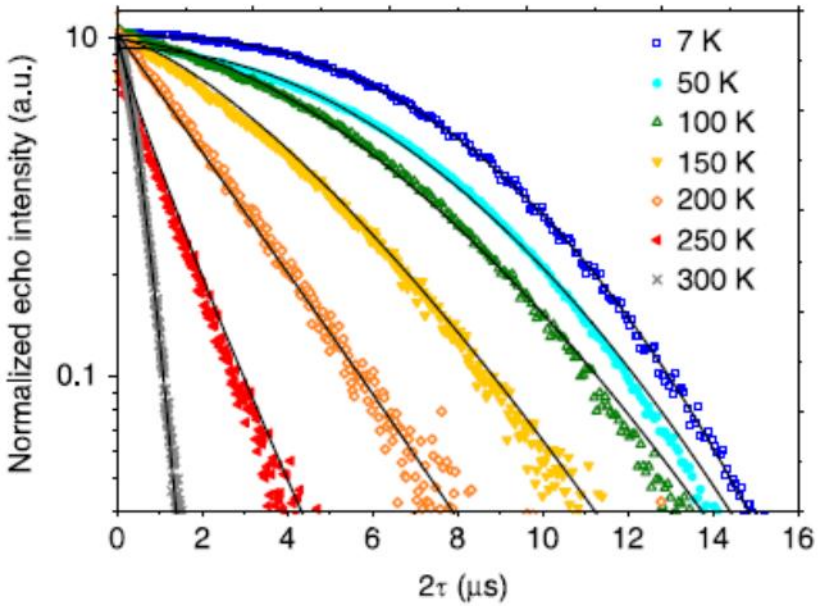

Figure 3 | Hahn echo decay curves at different temperatures for compound $\mathbf{1Cu_{0.001\%}}$. Integrated echo intensity normalized to the echo intensity immediately after the spectrometer deadtime as a function of delay between initial pulse and echo, at various temperatures as indicated. Solid lines are fits using equation (1), see text.

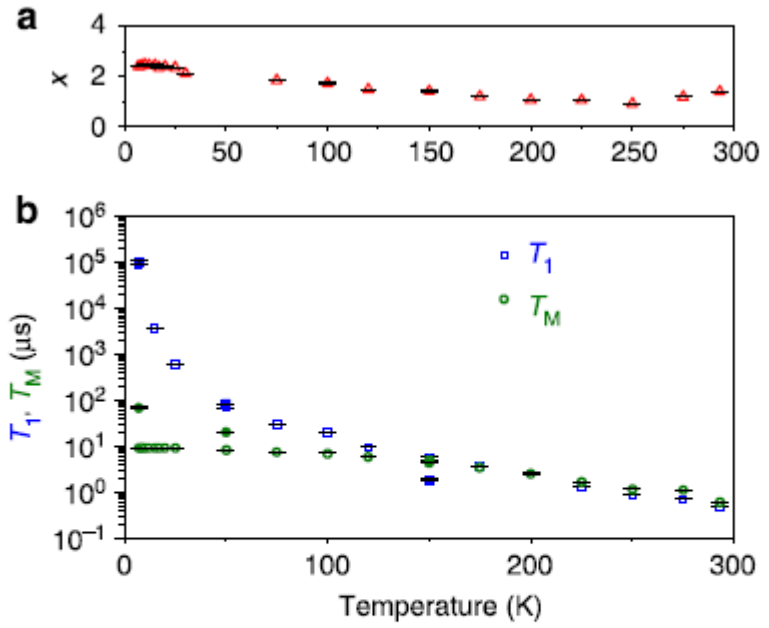

Figure 4 | Temperature dependence of electron spin relaxation times. (**a**) Stretch factor x as a function of temperature ($\mathbf{1Cu_{0.001\%}}$ only). (**b**) Spin–lattice relaxation (T_1) and phase memory time (T_M) as a function of temperature. Open symbols belong to $\mathbf{1Cu_{0.001\%}}$, filled symbols belong to $\mathbf{1Cu_{0.01\%}D}$. Error bars in all panels correspond to the s.d. of the fits.

Presence of a spin echo in an EPR experiment is an indicator of coherence. This data shows that the coherence is much better at very low temperatures, but that some coherence is maintained for a time of about 1 microsecond even at room temperature.

Methods Used in Room Temperature Copper Qubit Article

EPR measurements. CW X-Band EPR spectra were recorded on a Bruker EMX spectrometer ($\nu = 9.47$ GHz, Stuttgart). Pulsed EPR measurements were performed with a Bruker Elexsys E580 at Q-band ($\nu = 34$ GHz, Frankfurt, $\mathbf{1Cu_{0.001\%}}$) and a home-built[44] pulsed Q-band spectrometer ($\nu = 35$ GHz, Stuttgart, $\mathbf{1Cu_{0.01\%}D}$ and $\mathbf{1Cu_{1.5\%}}$). Temperatures between 7 and 275 K were obtained with an Oxford Instruments CF935 continuous flow helium cryostat, room temperature measurements were done at ~294 K without external temperature regulation. Typical pulse lengths were 16 ns ($\pi/2$) and 32 ns (π) (Frankfurt) and 20 ns ($\pi/2$) and 40 ns (π) (Stuttgart). For ESE-detected EPR spectra, the Hahn Echo pulse sequence ($\pi/2$—τ—π—τ—echo) with fixed delay times of $\tau = 140$ and 160 ns at 7 and 120 K, respectively, were applied under sweeping the magnetic field. Phase memory times were measured also with Hahn echo sequence, here at a fixed magnetic field under variation of the delay time τ. For measuring spin–lattice-relaxation times, the inversion recovery sequence (π—T—$\pi/2$—τ_{fix}—π—τ_{fix}—echo) with $\tau_{fix} = 140$ ns and phase cycling was applied. Nutation measurements were performed with a nutation pulse of variable length followed by a Hahn echo sequence (nutation pulse-τ_{nut}—$\pi/2$—τ_{fix}—π—τ_{fix}—echo) with $\tau_{nut} = 400$ ns, $\tau_{fix} = 140$ ns and different pulse powers.

Data analysis and simulation. ESE-detected spectra were simulated with EasySpin[45]. Errors of fit parameters (g and hyperfine values) were estimated by eye. T_M relaxation data were normalized to the first measurement point and fitted with Origin, indicated deviations correspond to the standard errors. Phase memory times (T_M) were extracted from fitting (stretched) exponentials, equation (1), to the Hahn echo decay curves. Experimental data of inversion recovery were fitted with a biexponential function for 7–25 K (fast and slow components) and for higher temperatures mono-exponential fits were applied.

Energy Conversion Table

	hartree	eV	cm^{-1}	kcal/mol	kJ/mol	^oK	J	Hz
hartree	1	27.2107	219 474.63	627.503	2 625.5	315 777.	43.60×10^{-19}	$6.57966 \times 10^{+15}$
eV	0.0367502	1	8 065.73	23.060 9	96.486 9	11 604.9	$1.602\ 10 \times 10^{-19}$	$2.418\ 04 \times 10^{+14}$
cm^{-1}	$4.556\ 33 \times 10^{-6}$	$1.239\ 81 \times 10^{-4}$	1	0.002 859 11	0.011 962 7	1.428 79	$1.986\ 30 \times 10^{-23}$	$2.997\ 93 \times 10^{+10}$
kcal/mol	0.001 593 62	0.043 363 4	349.757	1	4.18400	503.228	6.95×10^{-21}	$1.048\ 54 \times 10^{+13}$
kJ/mol	0.000 380 88	0.010 364 10	83.593	0.239001	1	120.274	1.66×10^{-21}	$2.506\ 07 \times 10^{+12}$
^oK	0.000 003 166 78	0.000 086 170 5	0.695 028	0.001 987 17	0.008 314 35	1	$1.380\ 54 \times 10^{-23}$	$2.083\ 64 \times 10^{+10}$
J	$2.294 \times 10^{+17}$	$6.241\ 81 \times 10^{+18}$	$5.034\ 45 \times 10^{+22}$	$1.44 \times 10^{+20}$	$6.02 \times 10^{+20}$	$7.243\ 54 \times 10^{+22}$	1	$1.509\ 30 \times 10^{+33}$
Hz	$1.519\ 83 \times 10^{-16}$	$4.135\ 58 \times 10^{-15}$	$3.335\ 65 \times 10^{-11}$	$9.537\ 02 \times 10^{-14}$		$4.799\ 30 \times 10^{-11}$	$6.625\ 61 \times 10^{-34}$	1